

CONFIDENTIAL NASA TM X-247

NASA TM X-247

GROUP [REDACTED]
int [REDACTED] ad
[REDACTED]



1N-34
380481

TECHNICAL MEMORANDUM

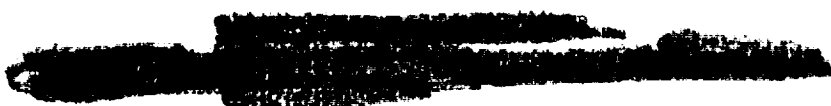
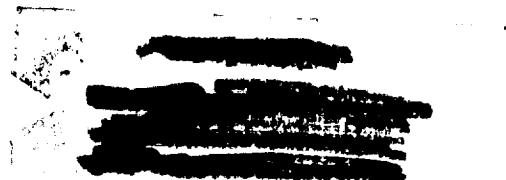
X-247

Declassified by authority of NASA
Classification Change Notices No. 143
Dated **2/4/68

PRELIMINARY HEAT-TRANSFER MEASUREMENTS ON A HYPERSONIC
GLIDE CONFIGURATION HAVING 79.5° SWEEPBACK AND
45° DIHEDRAL AT A MACH NUMBER OF 4.95

By P. Calvin Stainback

Langley Research Center
Langley Field, Va.



NATIONAL AERONAUTICS AND SPACE ADMINISTRATION
WASHINGTON February 1960



CONFIDENTIAL

NATIONAL AERONAUTICS AND SPACE ADMINISTRATION

TECHNICAL MEMORANDUM X-247

PRELIMINARY HEAT-TRANSFER MEASUREMENTS ON A HYPERSONIC
GLIDE CONFIGURATION HAVING 79.5° SWEEPBACK AND
45° DIHEDRAL AT A MACH NUMBER OF 4.95*

By P. Calvin Stainback

SUMMARY

An experimental investigation was conducted to evaluate the heat-transfer characteristics of a hypersonic glide configuration having 79.5° of sweepback (measured in the plane of the leading edges) and 45° of dihedral. The tests were conducted at a nominal Mach number of 4.95 and a stagnation temperature of 400° F. The test-section unit Reynolds number was varied from 1.95×10^6 to 12.24×10^6 per foot.


The results indicated that the laminar-flow heat-transfer rate to the lower surface of the model decreased as the distance from the ridge line increased except for thermocouples located near the semispan at an angle of attack of 0° with respect to the plane of the leading edges. The heat-transfer distribution (local heating rate relative to the ridge-line heating rate) was similar to the theoretical heat-transfer distribution for a two-dimensional blunt body, if the ridge line was assumed to be the stagnation line, and could be predicted by this theory provided a modified Newtonian pressure distribution was used. Except in the vicinity of the apex, the ridge-line heat-transfer rate could also be predicted from two-dimensional blunt-body heat-transfer theory provided it was assumed that the stagnation-line heat-transfer rate varied as the cosine of the effective sweep (sine of the angle of attack of the ridge line).

The heat-transfer level on the lower surface and the nondimensional heat-transfer distribution around the body on the lower surface were in qualitative agreement with the results of a geometric study of highly swept delta wings with large positive dihedrals made in reference 1.

INTRODUCTION

In a recent paper (ref. 1), a geometric study was made to determine some of the effects of dihedral on the leading-edge heat-transfer rate

*Title, Unclassified.



to swept delta wings. The results of this study indicated that the use of large positive dihedral on highly swept delta wings could shift the stagnation-line heat-transfer problem from the leading edge to the axis of symmetry (ridge line). Furthermore, a reduction in the stagnation-line heat-transfer rate could be expected since this shift in stagnation-line location could result in an increase in the characteristic dimension governing heating rates.

In reference 1, a configuration was proposed which would exploit the dihedral effects. It is the purpose of the present paper to present the heat-transfer measurements made for this configuration and to evaluate the predictions presented in the reference.

The configuration tested had a 79.5° sweepback angle measured in the plane of the leading edges, and a 45° dihedral angle measured in a plane perpendicular to the ridge line. The investigation was conducted at a nominal test-section Mach number of 4.95 and a stagnation temperature of 400° F. The test-section unit Reynolds number was varied from 1.95×10^6 to 12.24×10^6 per foot. The angle of attack, with respect to the plane of the leading edges, was varied from 0° to 20° .

SYMBOLS

c_m	specific heat of model material
h	model height
l	model length
M	free-stream Mach number
m	molecular weight
N_{Re}	unit Reynolds number
p	local static pressure
p_t'	stagnation pressure behind a normal shock
p_∞	free-stream static pressure
q	aerodynamic heating rate
q_s	storage heating rate

$$R = \frac{R_0}{m}$$

- R_0 universal gas constant
- r radius
- S model span
- T temperature
- t time
- U_∞ free-stream velocity
- u local velocity
- X coordinate axis along ridge line
- X' coordinate axis along upper-surface center line
- x, x', y, y' distance along corresponding coordinate axis
- Y coordinate axis around body from ridge line to semispan
- Y' coordinate axis around body from center line of upper surface to semispan
- α' angle of attack with respect to plane of the leading edges
- Γ dihedral angle, measured in plane perpendicular to ridge line
- ϵ_n angle between ridge line and plane of the leading edges
- ϵ_0 angle between leading edge and ridge line, panel semiapex angle
- ϵ_p half of angle between leading edges, plan-form semiapex angle
- θ Newtonian flow turning angle
- Λ_p plan-form sweep, complement of ϵ_p
- ρ_m density of model material



τ thickness of model skin

μ absolute viscosity

$$\omega = \frac{\mu}{RT}$$

Subscripts:

c indicates constant values of θ

e outer edge of boundary layer

le leading edge

n nose

r ridge line

sl stagnation-line value

t stagnation condition

th theoretical value

MODEL, TEST PROCEDURE, AND REDUCTION OF DATA

Model

The model was fabricated from 0.037-inch Inconel sheet stock; the model dimensions are given in the following table:

Length, l , in.	6.50
Span, S , in.	3.22
Height, h , in.	1.40
Angle between leading edge and ridge line, panel semiapex angle (ref.) ϵ_0 , deg	15
Angle between plane of leading edge and ridge line, ϵ_n , deg	10.7
Half of angle between leading edges, plan-form semiapex angle, ϵ_p , deg	10.5
Dihedral angle, Γ , deg	45
Leading-edge radius, r_{le} , in.	0.047
Ridge-line radius (constant over l) r_r , in.	0.50
Nose leading-edge radius, r_n , in.	0.094



The model was instrumented with a total of thirty-one 0.010-inch diameter (no. 30) iron-constantan thermocouples. The thermocouples were located on the ridge line, the center line of the plane of the leading edges, and two stations normal to the ridge line located 2.60 ($x/l = 0.400$) and 5.20 ($x/l = 0.800$) inches from the apex of the model. The locations of the individual thermocouples are noted on figure 1.

Test Procedure

Testing of the model was conducted in the gas dynamics laboratory of the Langley Research Center in a 9-inch axially symmetric blowdown jet at a nominal Mach number of 4.95 and a stagnation temperature of 400° F. The test-section Reynolds number for the investigation ranged from 1.95×10^6 to 12.24×10^6 per foot.

Testing was performed by the transient-heating method. This was accomplished by bringing the jet to the desired operating condition with the model outside the test section. After steady operation was obtained, a vertical door in the test section retracted and the isothermal model (at approximately room temperature), which was mounted on a second door actuated by a horizontal pneumatic cylinder, was inserted into the test section. The time between the instant that the model was just entering the test-section door and the instant that the model was in its proper location in the test section was 0.05 second. The model was removed from the test section after about 4 seconds.

A more complete description of the jet and this method of testing can be found in references 2 and 3.

Reduction of Data

Heat-transfer data were obtained by recording the temperature-time history of the model on a multichannel oscillograph. The aerodynamic heat-transfer rate can be calculated from the heat-storage rate if it can be demonstrated that lateral conduction and radiation effects are negligible and that normal conduction is essentially infinite. If the data are reduced for small times after the initial temperature rise, it is known (refs. 2 and 3) that lateral-conduction effects are small and that normal conduction is sufficiently large. Because of the low absolute temperature involved, the effects of radiation are small. Therefore, the aerodynamic heat-transfer rate is given by

$$q = q_s = \rho_m c_m \tau \frac{\partial T}{\partial t} \quad (1)$$



The change in temperature with respect to time used in the above equation was obtained by measuring the slope of the temperature-time curve at 0.25 second after the initial temperature rise. The model-wall thickness was taken to be equal to the nominal thickness of the sheet stock (0.037 in.) from which the model was formed. After the investigation was completed, the model was cut apart and the skin thickness was measured at several random locations. It was found that the skin thickness was actually 0.036 ± 0.0005 inch. The manufacturer's recommended value of 518.4 lb/cu ft was used for the model material density. Variation of the specific heat of the model material with temperature was obtained from reference 4.


The heat-transfer results are presented in terms of nondimensional heat-transfer ratios. In order to evaluate the heat-transfer distribution around the body at stations A and B, the local heat-transfer rate was divided by the corresponding ridge-line heat-transfer rate. It is noted that the ridge-line thermocouple for station A failed during the investigation. In order to evaluate the distribution under this condition, the ridge-line heat-transfer variation with model length was plotted, and a curve was fitted to the data. The value read from these curves at station A ($x/l = 0.400$) was used to form the heat-transfer ratio.

The ridge-line (stagnation-line) heat-transfer level was evaluated by forming a ratio between the ridge-line heat-transfer data and the theoretical stagnation-line heating rate to a swept circular cylinder with a radius equal to the model ridge-line radius. The theoretical heat-transfer rate for the cylinder at zero sweep was calculated from the results of reference 5. The stagnation-line heating rate was assumed to vary as the cosine of the effective sweep (see ref. 6) (sine of the angle of attack of the ridge line). The theoretical heat-transfer values are listed in table I for reference.

The data were reduced to the heat-transfer-ratio form because the recovery temperature around the model could not be accurately determined. It is noted, however, that the model was essentially isothermal as a result of the small temperature rise experienced ($5^{\circ} \text{ F} < \Delta T < 13^{\circ} \text{ F}$) at the time data were reduced. Since the model is essentially at isothermal conditions, the heat-transfer rate and the aerodynamic heat-transfer coefficient are qualitatively similar except for the variation of the recovery temperature on the model.

DISCUSSION OF RESULTS

In figure 2, the heat-transfer ratio q/q_{sl} for the lower surface at stations A and B is presented as a function of the dimensionless



distance from the ridge line y/r for the model for several values of the unit Reynolds number and angles of attack. By neglecting transition which apparently occurred on the model and which will be discussed more fully subsequently, it can be seen that the laminar-flow heat-transfer rate to the lower surface of the model decreased as the distance from the ridge line increased except for thermocouples located near the semi-span at an angle of attack of $\alpha' = 0^\circ$. The heat-transfer distribution (local heating rate relative to the ridge-line heating rate) is similar to the theoretical heat-transfer distribution for a two-dimensional blunt body of the same cross section if it is assumed that the ridge line is the stagnation line. As a result of this similarity, it appeared to be reasonable to attempt a correlation based on the cross-flow concept and on two-dimensional blunt body theory.

The theoretical curves presented in figure 2 were calculated from the following equation which can be obtained from the results of reference 7 for a two-dimensional blunt body

$$\frac{q}{q_{sl}} = \frac{F(s)}{\sqrt{\frac{1}{U_\infty} \left(\frac{du_e}{dy} \right)_{y=0}}} \quad (2)$$

where

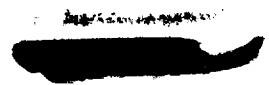
$$F(s) = \frac{\frac{1}{\sqrt{2}} \frac{p}{p_{t'}} \frac{\omega_e}{\omega_{e,sl}} \frac{u_e}{U_\infty}}{\left(\int_0^y \frac{p}{p_{t'}} \frac{u_e}{U_\infty} \frac{\omega_e}{\omega_{e,sl}} dy \right)^{1/2}} \quad (3)$$

For a two-dimensional blunt body with a circular cylinder for a leading edge, the above equation can be reduced to

$$\frac{q}{q_{sl}} = \frac{\frac{1}{\sqrt{2}} \frac{p}{p_{t'}} \theta}{\left[\int_0^\theta \left(\frac{p}{p_{t'}} \right)^\theta d\theta \right]^{1/2}} \quad (4)$$

provided the following assumptions are made:

$$\frac{u_e}{U_\infty} = \frac{1}{U_\infty} \left(\frac{du_e}{d\theta} \right)_{\theta=0} \theta; \quad \frac{\omega_e}{\omega_{e,sl}} \approx 1$$



The pressure variations required for calculating the theoretical curves were assumed to be the modified Newtonian pressure distribution given as

$$\frac{p}{p_t'} = \cos^2 \theta + \frac{p_\infty}{p_t'} \sin^2 \theta \quad (5)$$

Substituting equation (5) into equation (4) and integrating gives the following:

For $\theta = 0$ (stagnation line) to $\theta = 0.785$ radian (tangency point),

$$\frac{q}{q_{sl}} = \frac{2\theta \left(\cos^2 \theta + \frac{p_\infty}{p_t'} \sin^2 \theta \right)}{\left[(2\theta^2 + 2\theta \sin 2\theta + \cos 2\theta - 1) + \frac{p_\infty}{p_t'} (2\theta^2 - 2\theta \sin 2\theta - \cos 2\theta + 1) \right]^{1/2}} \quad (6a)$$

and for $\theta > 0.785$ radian

$$\frac{1}{q_{sl}} = \frac{2\theta_c \left(\cos^2 \theta_c + \frac{p_\infty}{p_t'} \sin^2 \theta_c \right)}{\left[(2\theta_c^2 + 2\theta_c \sin 2\theta_c + \cos 2\theta_c - 1) + \frac{p_\infty}{p_t'} (2\theta_c^2 - 2\theta_c \sin 2\theta_c - \cos 2\theta_c + 1) + 8\theta_c \left(\cos^2 \theta_c + \frac{p_\infty}{p_t'} \sin^2 \theta_c \right) \left(\frac{\gamma}{\gamma - 1} - \theta_c \right) \right]^{1/2}} \quad (6b)$$

The curve noted as "Lees + Newtonian pressure distribution" in figure 2 was computed by using the Mach number normal to the ridge line to evaluate the pressure ratio p_∞/p_t' in equation (5). (This procedure was noted as Newtonian II in ref. 8.) The pressure on the wing panel (lower surface) after the line of tangency is, of course, constant for this method.

The curve noted as "Lees + measured pressure data" in figure 2 was computed by modifying the quantity p_∞/p_t' in equation (5) to force the equation to agree with the measured pressure ratio p/p_t' at the line of tangency ($\theta = 0.785$ radian) as given in reference 8. This pressure variation was assumed to exist over the region between the ridge line and the line of tangency. On the wing panel where θ is constant, a straight line was fitted to the pressure data (ref. 8). These relationships for the pressure ratio computed in this manner were substituted into equations (2) and (3) to calculate the heat-transfer ratio. The required velocity ratio was obtained from the measured pressure ratio by assuming that the flow about the model from the stagnation line was isentropic. The quantity $\omega_e/\omega_{e,sl}$ was again assumed to be unity.

From figure 2 it can be seen that the agreement between the theoretical heat-transfer distributions, computed from either pressure distribution, and the measured heat-transfer distributions on the lower surface is fair for the angle-of-attack range investigated. Therefore, it appears reasonable to use the theoretical heat-transfer distribution of reference 7 in conjunction with the Newtonian pressure distribution obtained from the cross-flow concept as a method for calculating the heat-transfer distribution about the configuration provided x/l is at least equal to or greater than 0.400.


At the highest unit Reynolds number investigated, transition appeared to occur on the model as indicated in figure 2 by a rapid, localized increase in the heating rate. From the limited amount of transition data available, the transition Reynolds number, based on free-stream conditions and normal distance from the ridge line, appeared to vary with angle of attack. This variation ranged from 0.715×10^6 at an angle of attack $\alpha' = 0^\circ$ to 0.369×10^6 at $\alpha' = 20^\circ$.

Also presented in figure 2 is the heat-transfer rate to the upper surface of the model. The laminar-flow heat-transfer rate to the upper surface at stations A and B was at least about 60 percent less than the heat-transfer rate to the ridge line except for an angle of attack $\alpha' = 0^\circ$.

Figure 3 presents the ratio of the measured stagnation-line heat-transfer rate to the theoretical value, $q_{sl}/q_{sl,th}$, where $q_{sl,th}$ was calculated from the results of reference 5 and the cosine relationship of reference 6. The theoretical stagnation-line heat-transfer rates are tabulated in table I for reference. For most conditions investigated, the theoretical heat-transfer rate overestimated the heating rate to the ridge line except in the vicinity of the apex. This overestimation was as much as 35 percent, but the average was of the order of 15 percent. The high heating rate in the vicinity of the apex agrees with the trend which could be predicted from the measured pressure data of reference 8.

Figure 3 also presents the ratio of the heat-transfer rate to the center line of the upper surface of the model to the theoretical ridge-line (stagnation-line) heat-transfer rate. The laminar-flow heat-transfer rate to the upper-surface center line was about 20 percent of the theoretical ridge-line heat-transfer rate except for an angle of attack $\alpha' = 0^\circ$.

The heat-transfer level on the lower surface and the nondimensional heat-transfer distribution around the body on the lower surface of the model are in qualitative agreement with the results of a geometric study made in reference 1 of highly swept delta wings with large positive dihedrals.



Because of the limited number of thermocouples installed on the upper surface of the model, no systematic variation of the heating rates to this surface could be discerned. In order to obtain further information on the heat-transfer rate to the model, an additional investigation was conducted which employed a temperature-sensitive-paint technique. The paint¹ used has a pronounced characteristic color change at a known temperature. These tests were conducted in a manner similar to the heat-transfer investigation. The models used for this investigation were made of plastic in order to reduce lateral conduction effects on the results.

The results of the temperature-sensitive-paint investigation are presented in figure 4. In figure 4(a) the model is shown coated with the temperature-sensitive paint prior to testing. In the succeeding figures the dark areas in the black and white photographs represent regions with higher heating rates than the light areas. Tests conducted at low angles of attack ($\alpha' = 0^\circ$ and 5°) indicated that the heating rate to the lower surface of the model was higher at both the ridge line and the semispan than to the other areas of the lower surface. (The high-temperature region at the semispan is not shown in figure 4(c) as a result of the effects of highlights on the photograph.) At $\alpha' = 10^\circ$, the highest heat-transfer rate occurred at the ridge line as shown in figure 4(d).


On the upper surface, the temperature-sensitive paint indicated that the apparent nonsystematic variation of the heating rate as determined by the thermocouples was caused, to some extent, by two localized high heating areas parallel to the center line and located approximately at the quarter span of the model. These high heating areas were apparently caused by a pair of vortices generated by the apex of the model.

The temperature-sensitive-paint investigation was conducted at a single, relatively low, unit Reynolds number. Because of this, it is possible that some of the apparent nonsystematic variation of the heating rate to the upper surface as noted during the heat-transfer investigation at higher unit Reynolds numbers might be due to transition and would not be disclosed by the temperature-sensitive-paint investigation.

CONCLUSIONS

An experimental investigation was conducted to evaluate the heat-transfer characteristics of a hypersonic glide configuration with 79.5°

¹The temperature-sensitive paint, which carried the trade name "Thermocolor" (presently sold under the label "DetectoTemp"), was procured from the Curtiss-Wright Corporation, Princeton Division.




of sweepback (measured in the plane of the leading edges) and 45° of dihedral. The tests were conducted at a nominal Mach number of 4.95 and a stagnation temperature of 400° F. The test-section unit Reynolds number was varied from 1.95×10^6 to 12.24×10^6 per foot.

The results indicated that the laminar-flow heat-transfer rate to the lower surface of the model decreased as the distance from the ridge line increased except for thermocouples located near the semispan at an angle of attack of 0° with respect to the plane of the leading edges. The heat-transfer distribution (local heating rate relative to the ridge-line heating rate) was similar to the theoretical heat-transfer distribution for a two-dimensional blunt body, if the ridge line was assumed to be the stagnation line, and could be predicted by this theory provided a modified Newtonian pressure distribution was used. Except in the vicinity of the apex, the ridge-line heat-transfer rate could also be predicted from two-dimensional blunt-body heat-transfer theory provided it was assumed that the stagnation-line heat-transfer rate varied as the cosine of the effective sweep (sine of the angle of attack of the ridge line).

The heat-transfer level on the lower surface and the nondimensional heat-transfer distribution around the body on the lower surface were in qualitative agreement with the results of a geometric study of highly swept delta wings with large positive dihedrals made in reference 1.

Langley Research Center,
National Aeronautics and Space Administration,
Langley Field, Va., September 3, 1959.



REFERENCES

1. Cooper, Morton, and Stainback, P. Calvin: Influence of Large Positive Dihedral on Heat Transfer to Leading Edges of Highly Swept Wings at Very High Mach Numbers. NASA MEMO 3-7-59L, 1959.
2. Cooper, Morton, and Mayo, Edward E.: Measurements of Local Heat Transfer and Pressure on Six 2-Inch-Diameter Blunt Bodies at a Mach Number of 4.95 and at Reynolds Number Per Foot Up to 81×10^6 . NASA MEMO 1-3-59L, 1959.
3. Stainback, P. Calvin: An Experimental Investigation at a Mach Number of 4.95 of Flow in the Vicinity of a 90° Interior Corner Aligned With the Free-Stream Velocity. NASA TN D-184, 1960.
4. O'Sullivan, William J., Jr.: Some Thermal and Mechanical Properties of Inconel at High Temperatures for Use in Aerodynamic Heating Research. Proc. A.S.T.M., vol. 55, 1955, pp. 757-763.
5. Reshotko, Eli, and Cohen, Clarence B.: Heat Transfer at the Forward Stagnation Point of Blunt Bodies. NACA TN 3513, 1955.
6. Feller, William V.: Investigation of Equilibrium Temperatures and Average Laminar Heat-Transfer Coefficients for the Front Half of Swept Circular Cylinders at a Mach Number of 6.9. NACA RM L55F08a, 1955.
7. Lees, Lester: Laminar Heat Transfer Over Blunt-Nosed Bodies at Hypersonic Flight Speeds. Jet Propulsion, vol. 26, no. 4, Apr. 1956, pp. 259-269.
8. Cooper, Morton, and Gunn, Charles R.: Pressure Measurements on a Hypersonic Glide Configuration Having 79.5° Sweepback and 45° Dihedral at a Mach Number of 4.95. NASA TM X-223, 1959.

TABLE I
THEORETICAL STAGNATION-LINE (RIDGE-LINE) HEAT-TRANSFER RATE

[$M = 4.95$; $T_t = 400^\circ \text{ F}$; $r = 0.50 \text{ in.}$]

N_{Re} per foot	$q_{sl,th}$, Btu/sec-ft ² , at -				
	$\alpha' = 0^\circ$	$\alpha' = 5^\circ$	$\alpha' = 10^\circ$	$\alpha' = 15^\circ$	$\alpha' = 20^\circ$
1.95×10^6	0.7466	1.0873	1.4198	1.7413	2.0497
3.39×10^6	.9932	1.4464	1.8886	2.3165	2.7267
6.34×10^6	1.3580	1.9778	2.5824	3.1675	3.7284
12.24×10^6	1.8868	2.7478	3.5879	4.4007	5.1800

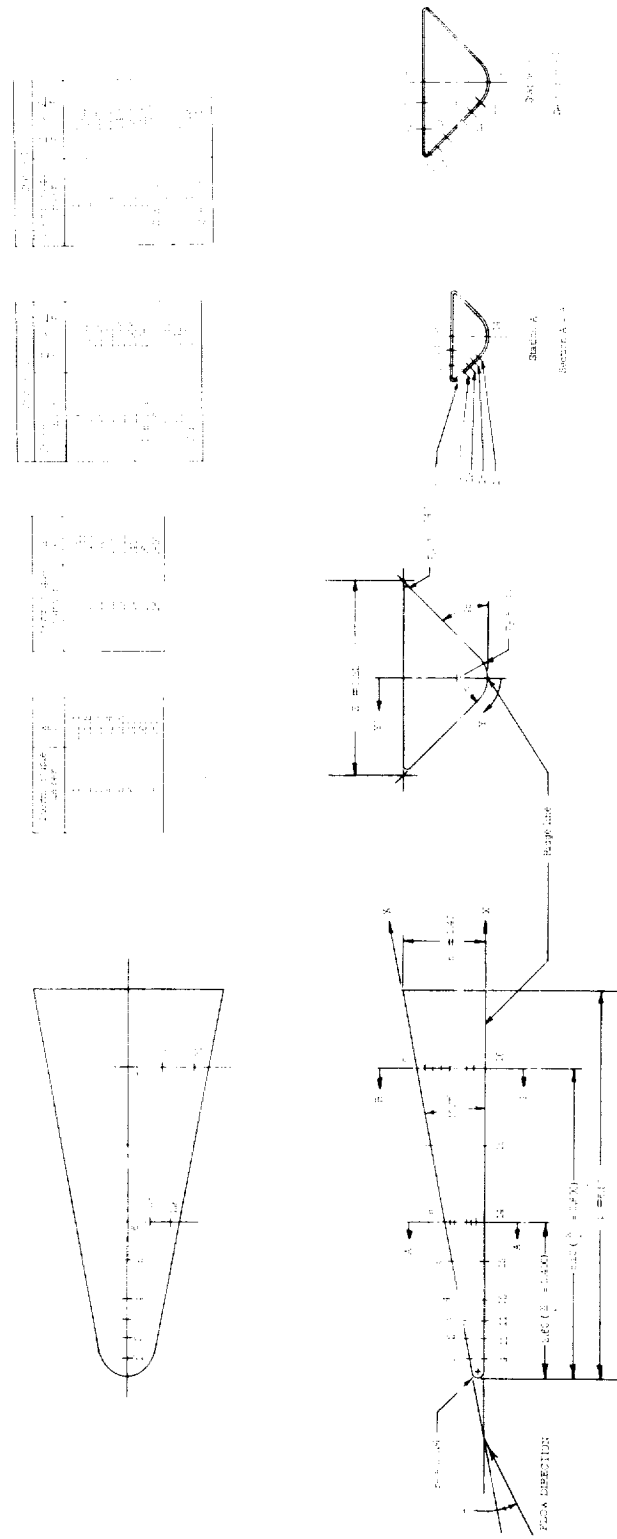
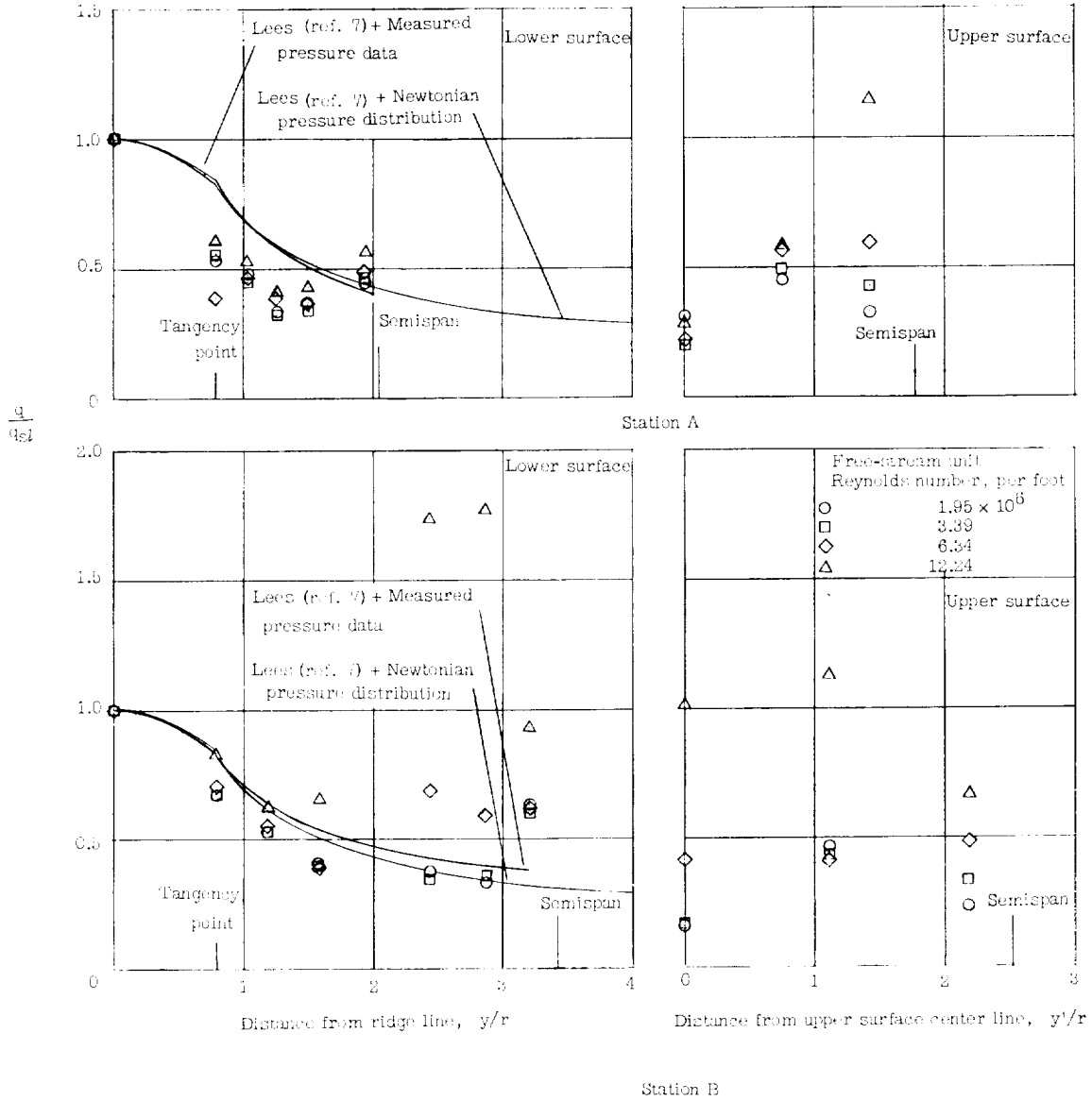
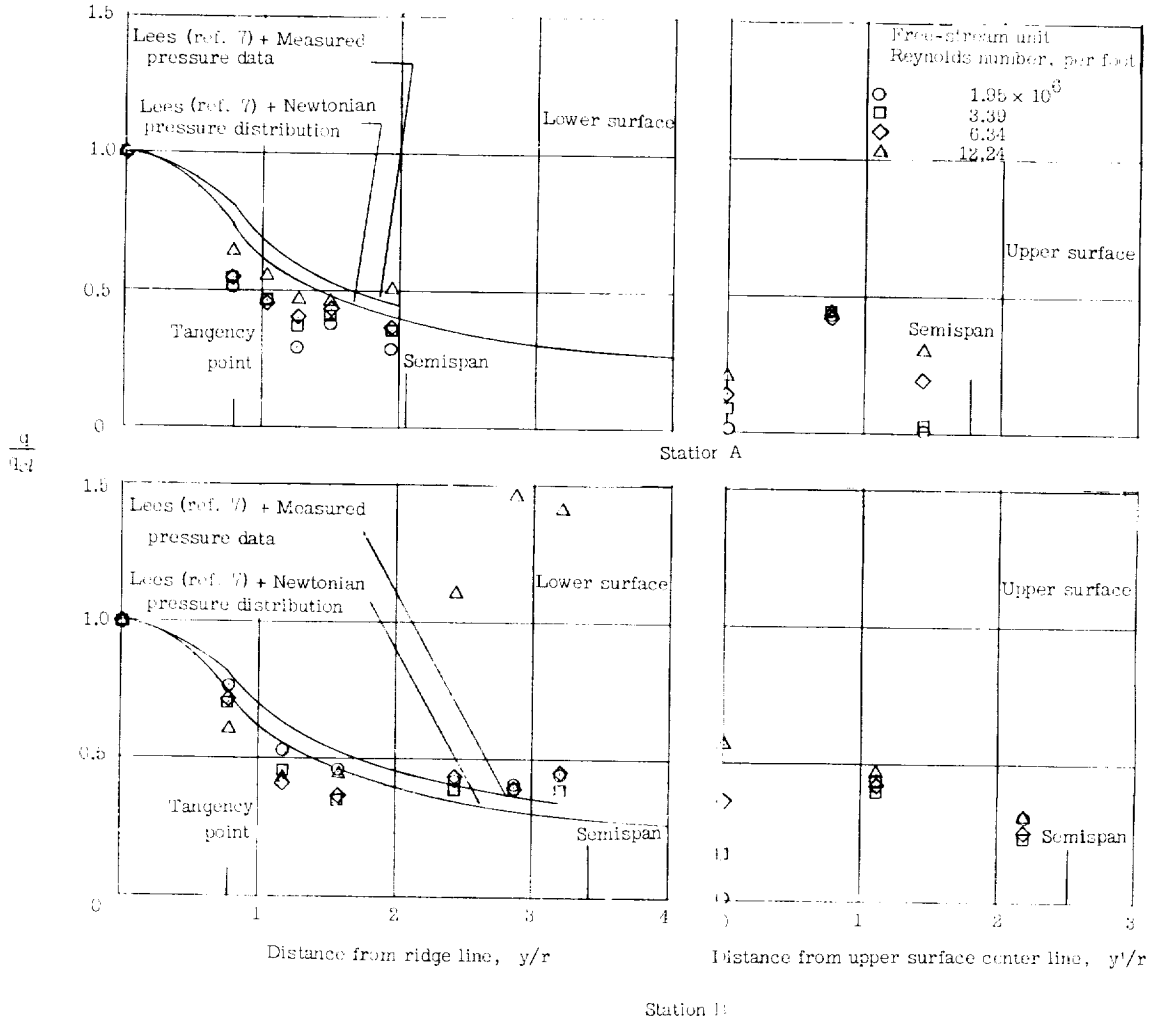


Figure 1.- Geometry and instrumentation of model. All dimensions are in inches.



(a) $\alpha' = 0^\circ$.

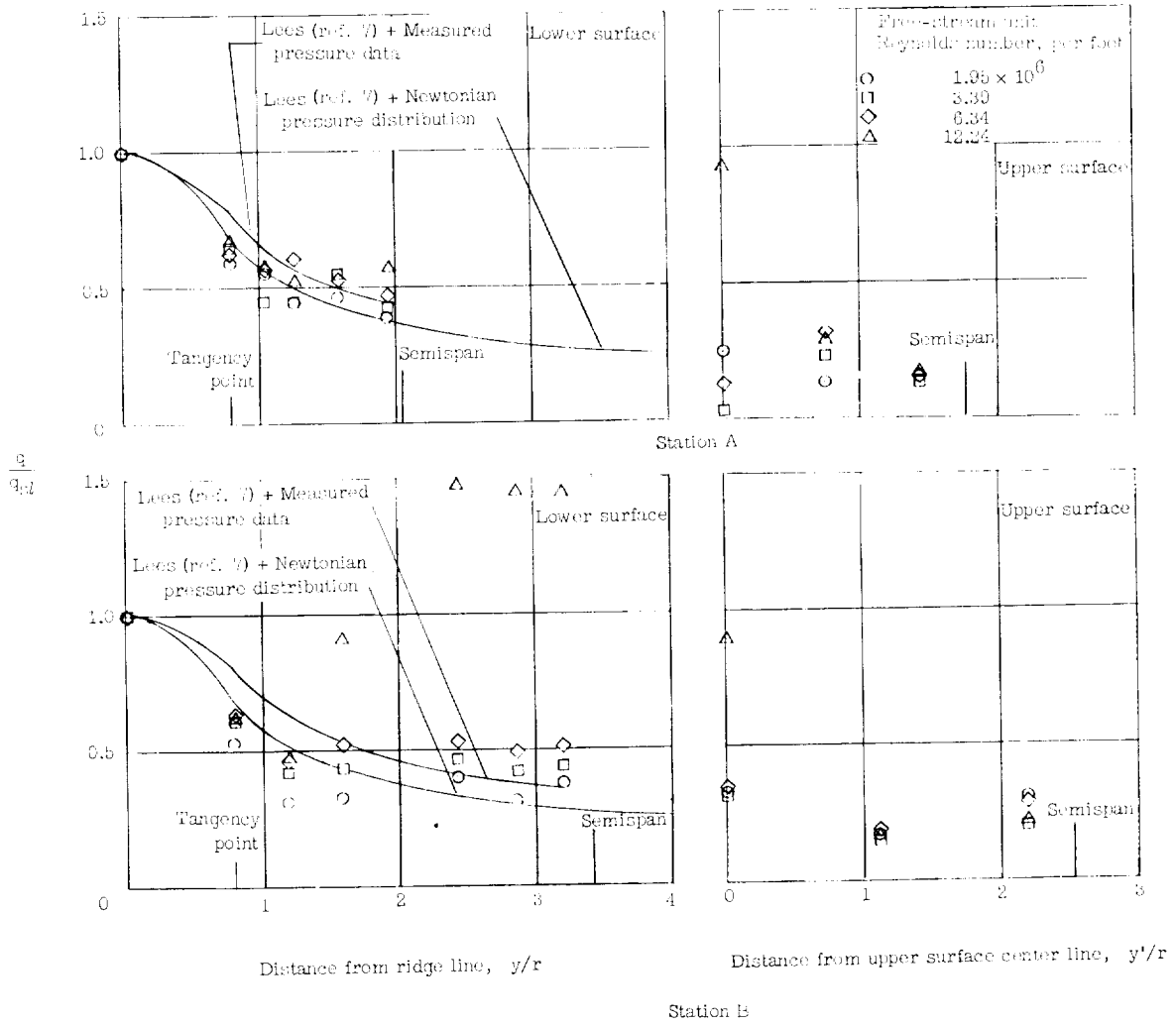
Figure 2.- Heat-transfer variation around model at stations A and B.



(b) $\alpha' = 5^\circ$.

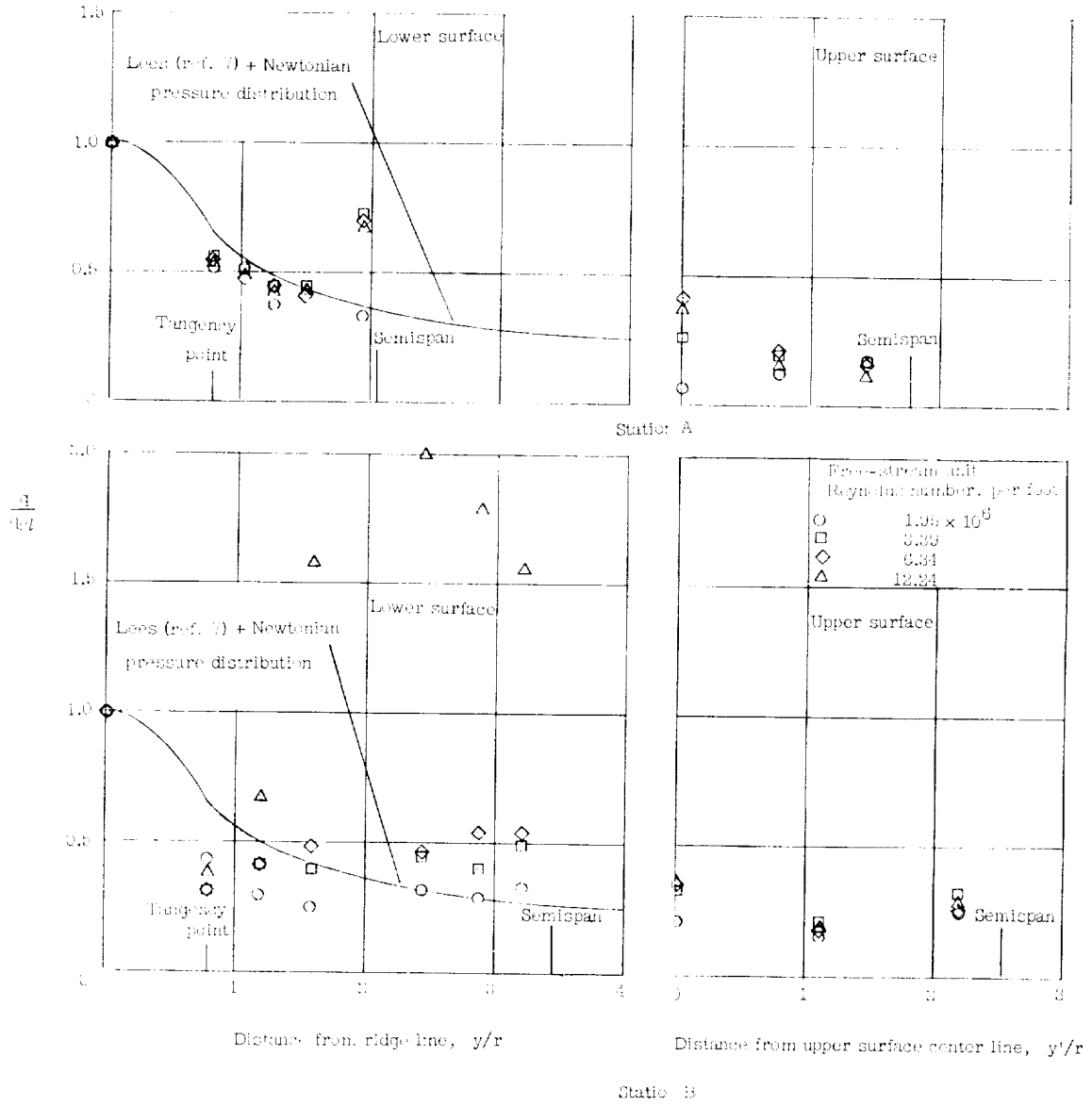
Figure 2.- Continued.





(c) $\alpha' = 10^\circ$.

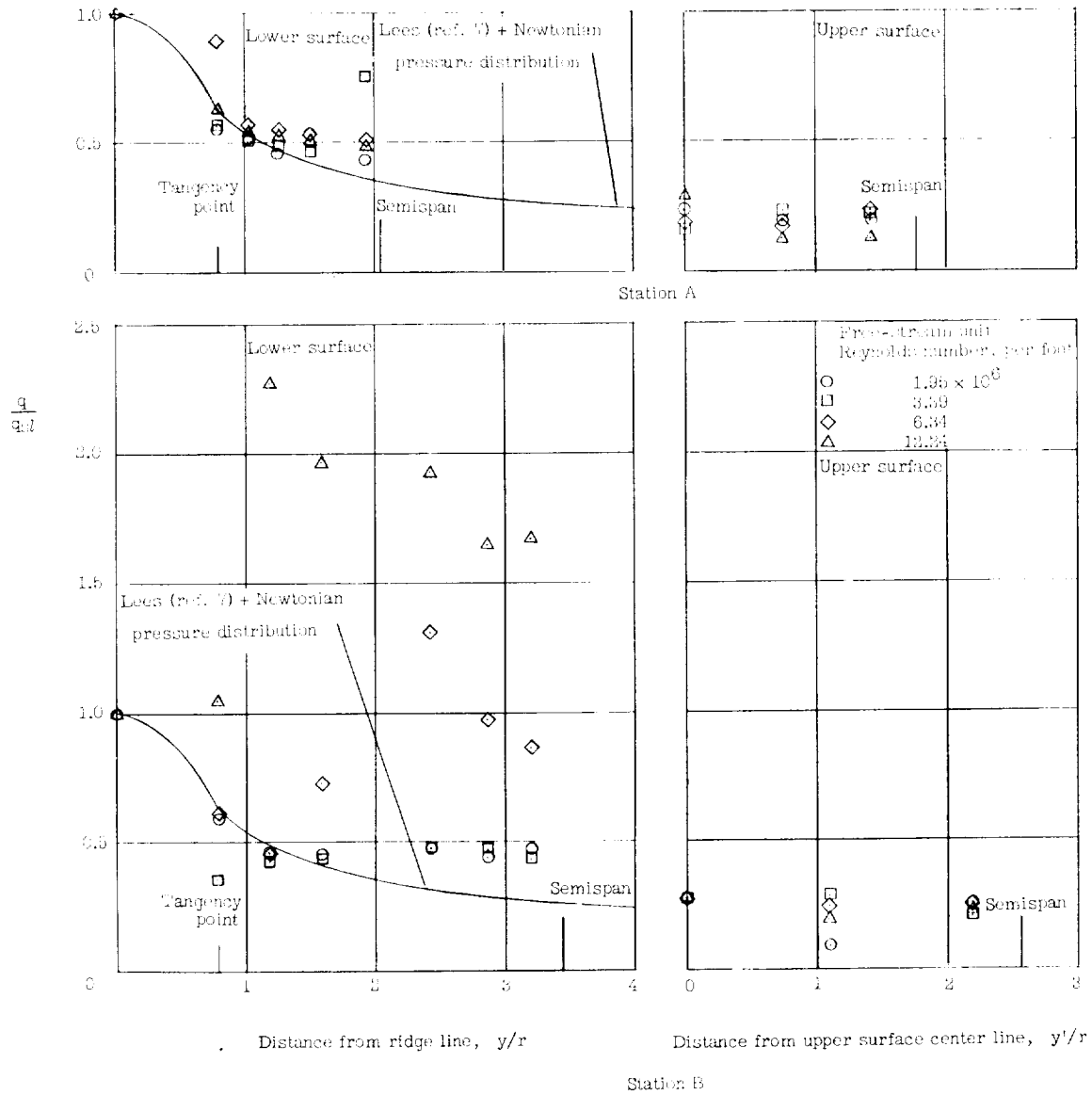
Figure 2.- Continued.



(d) $\alpha' = 15^\circ$.

Figure 2.- Continued.

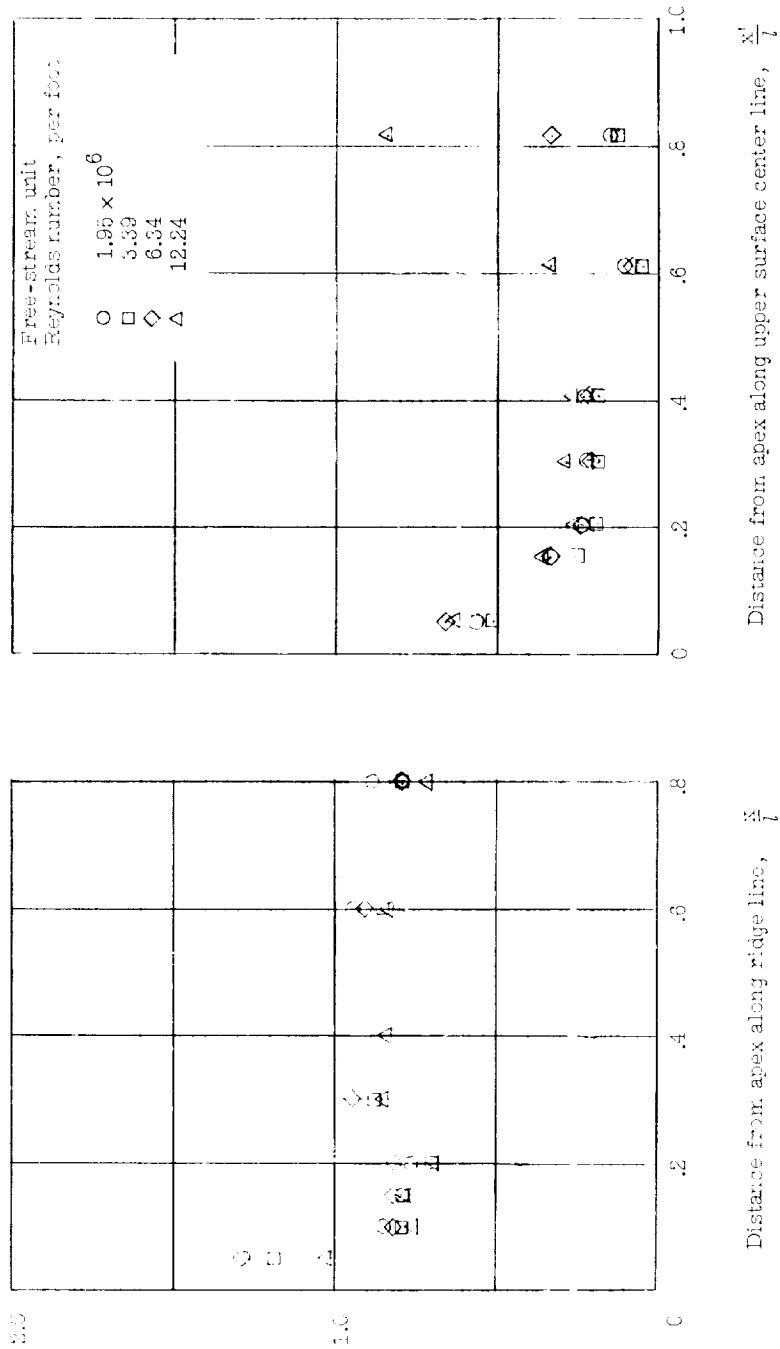




(e) $\alpha' = 20^\circ$.

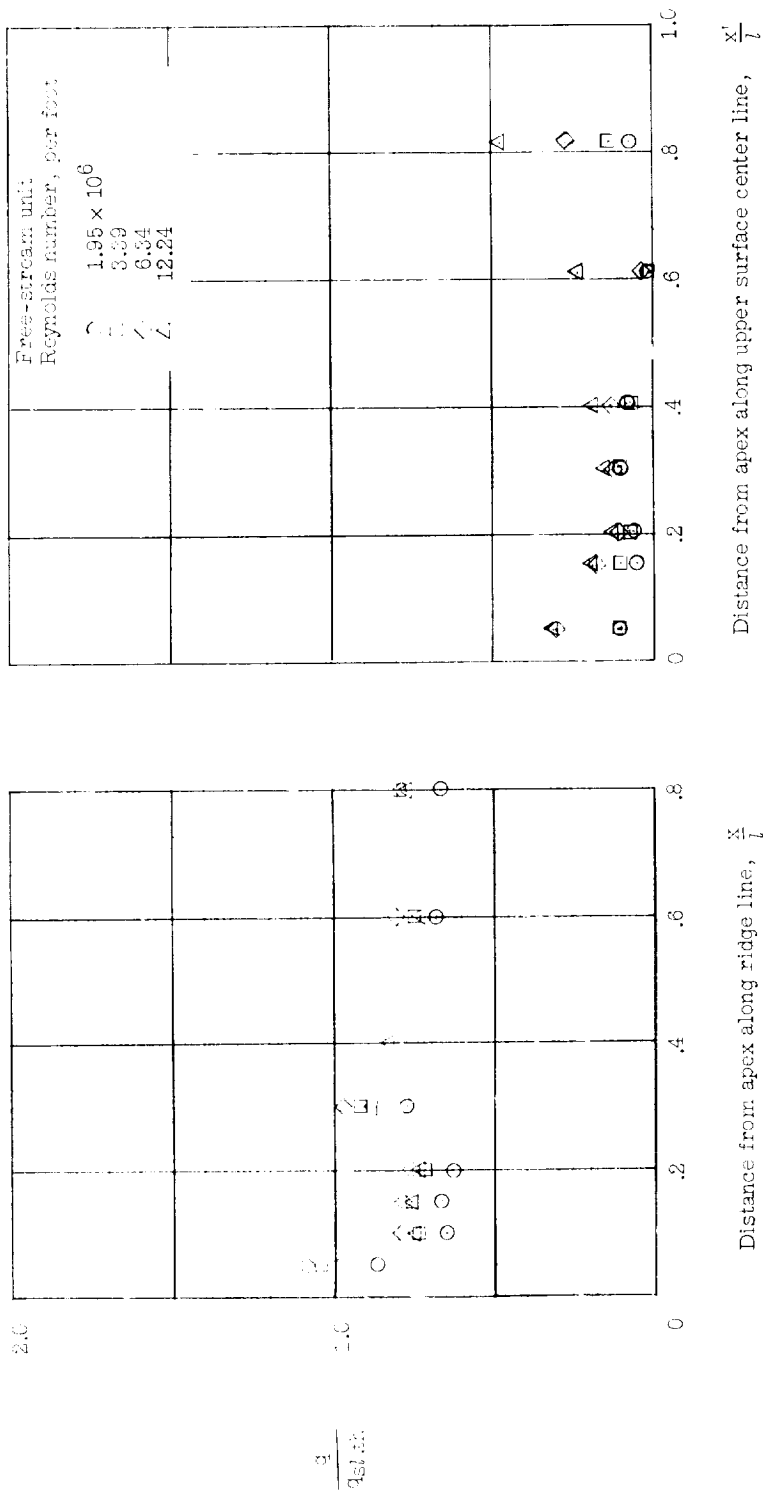
Figure 2.- Concluded.

CONFIDENTIAL



(a) $\alpha' = 0^\circ$.

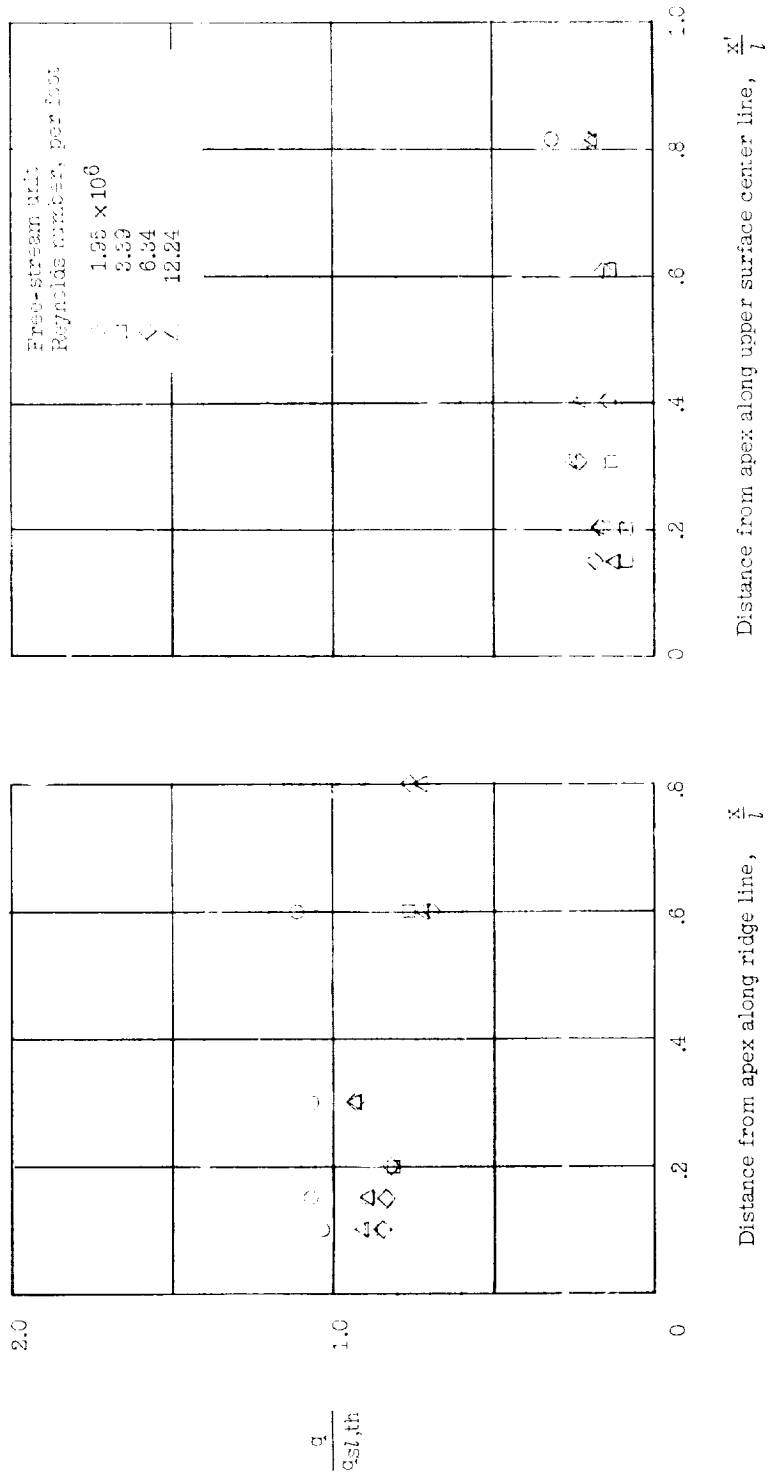
Figure 3.- Heat transfer to model along ridge line and upper-surface center line.



(b) $\alpha' = 5^\circ$.

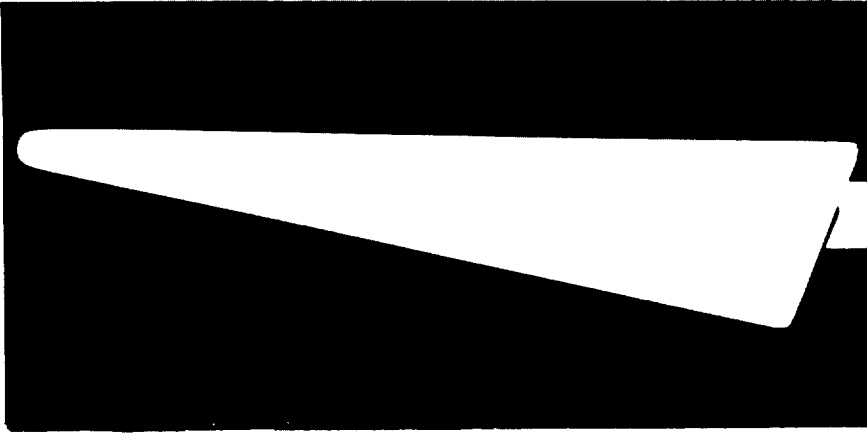
Figure 3.- Continued.

CONFIDENTIAL

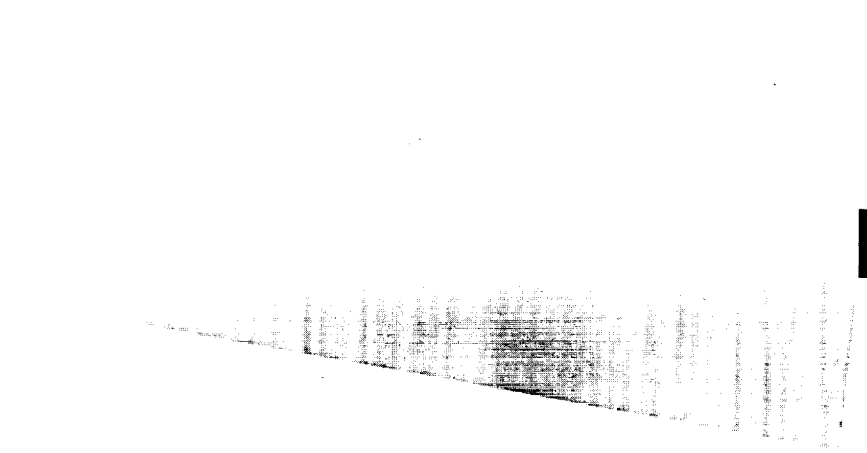


(e) $\alpha' = 20^\circ$.

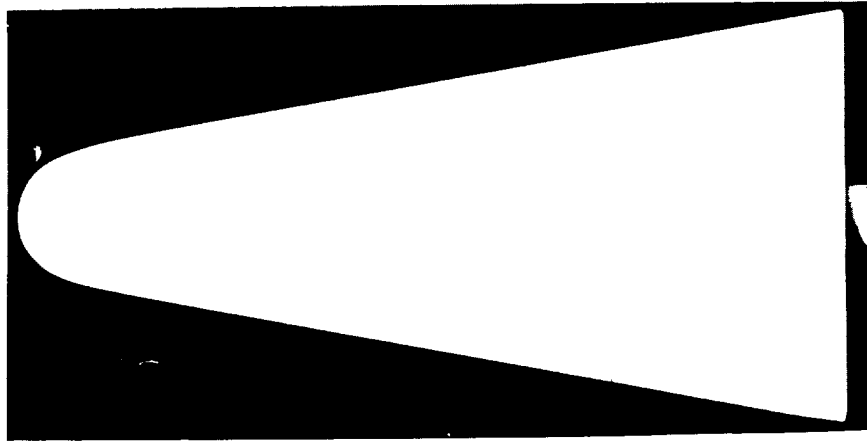
Figure 3.- Concluded.



Side view L-59-3791



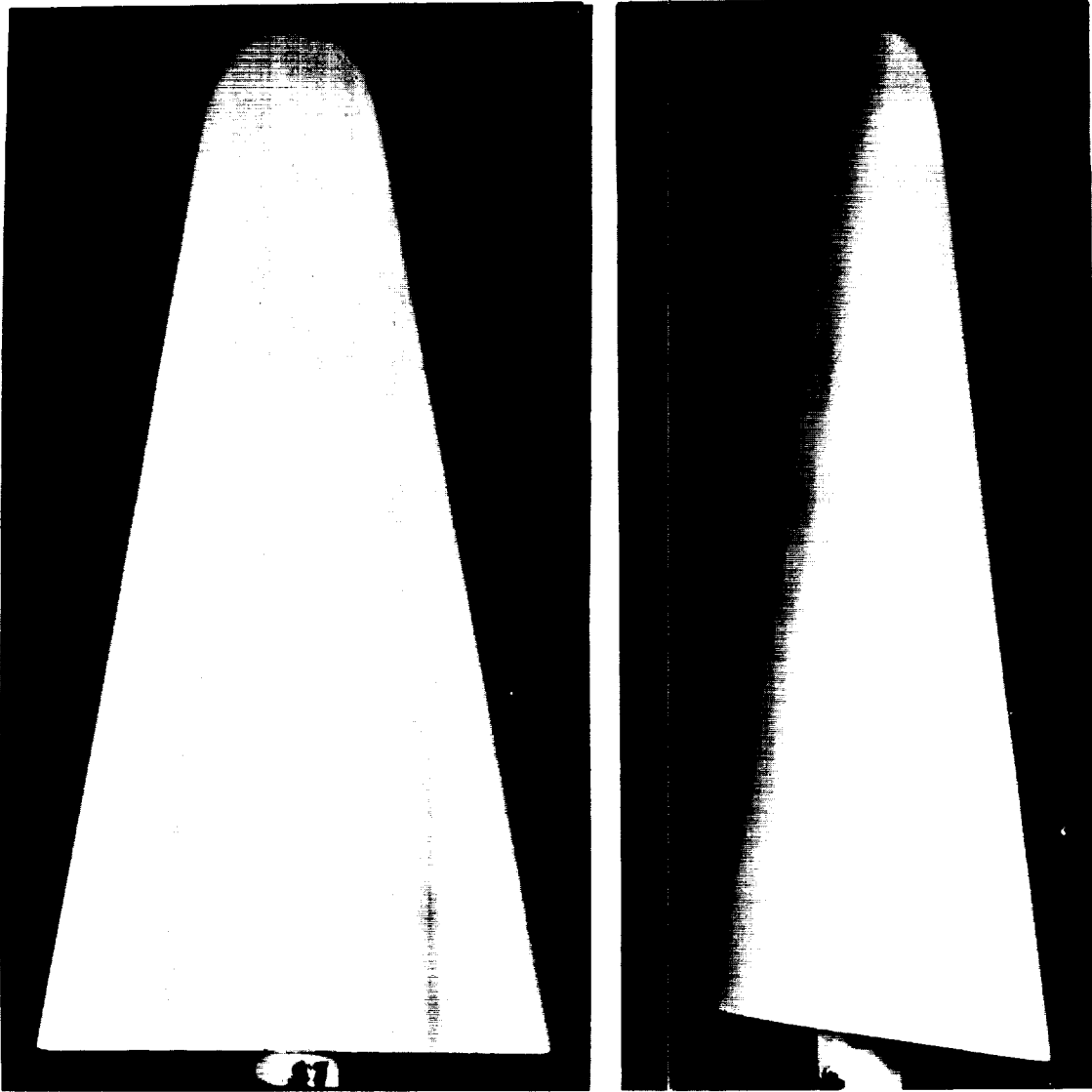
Lower surface L-59-3248



Upper surface L-59-3794

(a) Model painted with temperature-sensitive paint prior to testing.

Figure 4.- Results of temperature-sensitive-paint investigation with model.

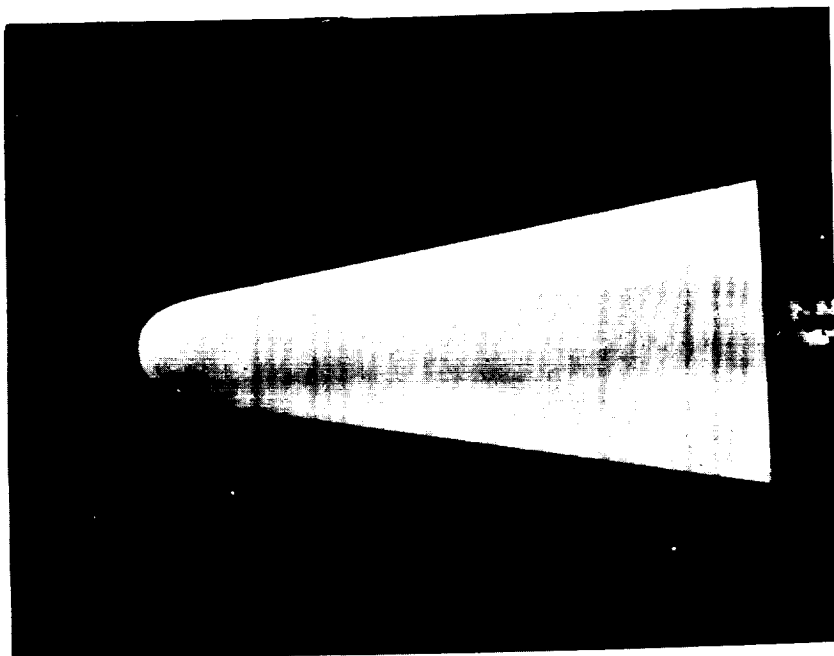


Upper surface L-59-3323

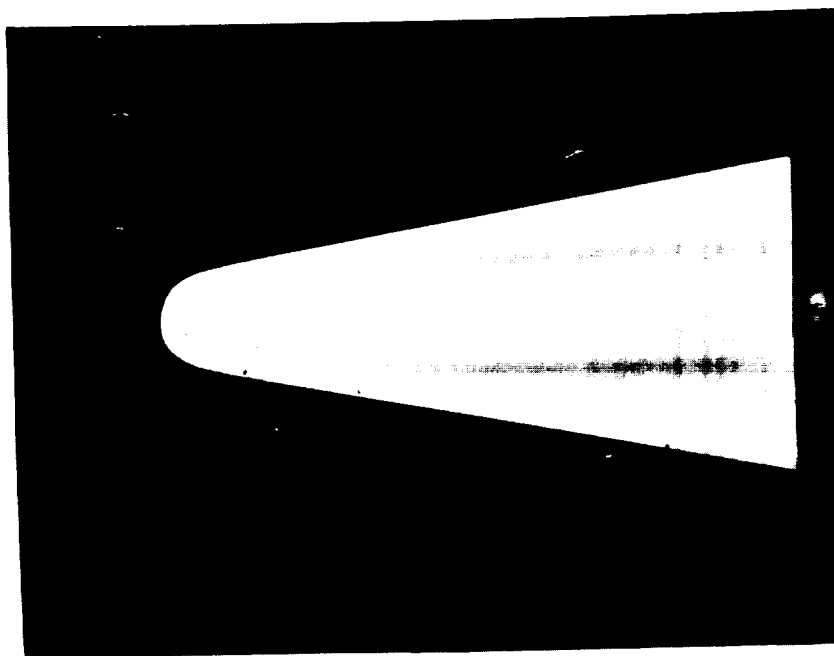
Side view L-59-3321

(b) Mach number = 4.95; angle of attack = 0° ;
unit Reynolds number = 3.39×10^6 per foot.

Figure 4.- Continued.

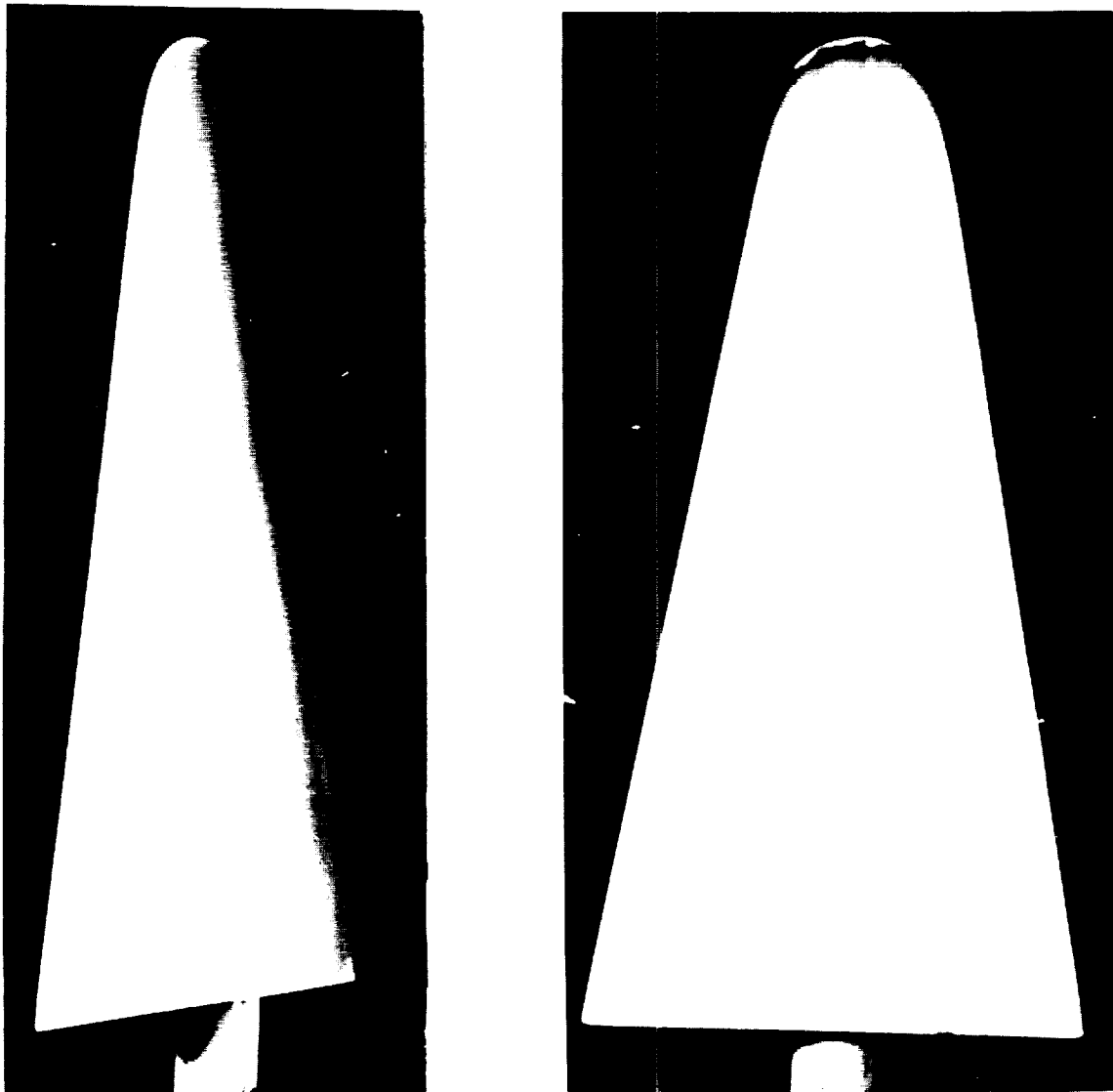


Lower surface L-59-2476



Upper surface L-59-2475

(c) Mach number = 4.95; angle of attack = 5° ; unit Reynolds number = 3.39×10^6 per foot.



Side view L-59-3347

Upper surface L-59-3346

(d) Mach number = 4.95; angle of attack = 10° ;
unit Reynolds number = 3.39×10^6 per foot.

Figure 4.- Concluded.

NASA TM X-247

National Aeronautics and Space Administration.
PRELIMINARY HEAT-TRANSFER MEASUREMENTS
ON A HYPERSONIC GLIDE CONFIGURATION HAVING
79.5° SWEEPBACK AND 45° DIHEDRAL AT A MACH
NUMBER OF 4.95. P. Calvin Stainback. February
1960. 28p. diags., photos., tab.
(NASA TECHNICAL MEMORANDUM X-247)

(Title, Unclassified)
An experimental investigation was conducted to evaluate the heat-transfer characteristics of the configuration. The tests were conducted at a nominal Mach number of 4.95 and a stagnation temperature of 400° F. The test-section unit Reynolds number was varied from 1.95×10^6 to 12.24×10^6 per foot. The heat-transfer distribution (local heating rate relative to the ridge-line heating rate) and the ridge-line heat-transfer level could be predicted by two-dimensional blunt-body theory for angles of attack greater than 0° provided it was assumed that the stagnation line was located on the ridge line.
Copies obtainable from NASA, Washington

1. Heat Transfer, Aerodynamic (1.1.4.2)
 2. Wings, Complete (1.2.2)
 3. Wings, Complete - Design Variables (1.2.2.2)
 4. Wings, Complete - Sweep (1.2.2.2.3)
 5. Dihedral - Complete Wings (1.2.2.2.7)
- I. Stainback, P. Calvin
II. NASA TM X-247

NASA

NASA TM X-247

National Aeronautics and Space Administration.
PRELIMINARY HEAT-TRANSFER MEASUREMENTS
ON A HYPERSONIC GLIDE CONFIGURATION HAVING
79.5° SWEEPBACK AND 45° DIHEDRAL AT A MACH
NUMBER OF 4.95. P. Calvin Stainback. February
1960. 28p. diags., photos., tab.
(NASA TECHNICAL MEMORANDUM X-247)

(Title, Unclassified)
An experimental investigation was conducted to evaluate the heat-transfer characteristics of the configuration. The tests were conducted at a nominal Mach number of 4.95 and a stagnation temperature of 400° F. The test-section unit Reynolds number was varied from 1.95×10^6 to 12.24×10^6 per foot. The heat-transfer distribution (local heating rate relative to the ridge-line heating rate) and the ridge-line heat-transfer level could be predicted by two-dimensional blunt-body theory for angles of attack greater than 0° provided it was assumed that the stagnation line was located on the ridge line.
Copies obtainable from NASA, Washington

1. Heat Transfer, Aerodynamic (1.1.4.2)
 2. Wings, Complete (1.2.2)
 3. Wings, Complete - Design Variables (1.2.2.2)
 4. Wings, Complete - Sweep (1.2.2.2.3)
 5. Dihedral - Complete Wings (1.2.2.2.7)
- I. Stainback, P. Calvin
II. NASA TM X-247

NASA

NASA TM X-247

National Aeronautics and Space Administration.
PRELIMINARY HEAT-TRANSFER MEASUREMENTS
ON A HYPERSONIC GLIDE CONFIGURATION HAVING
79.5° SWEEPBACK AND 45° DIHEDRAL AT A MACH
NUMBER OF 4.95. P. Calvin Stainback. February
1960. 28p. diags., photos., tab.
(NASA TECHNICAL MEMORANDUM X-247)

(Title, Unclassified)
An experimental investigation was conducted to evaluate the heat-transfer characteristics of the configuration. The tests were conducted at a nominal Mach number of 4.95 and a stagnation temperature of 400° F. The test-section unit Reynolds number was varied from 1.95×10^6 to 12.24×10^6 per foot. The heat-transfer distribution (local heating rate relative to the ridge-line heating rate) and the ridge-line heat-transfer level could be predicted by two-dimensional blunt-body theory for angles of attack greater than 0° provided it was assumed that the stagnation line was located on the ridge line.
Copies obtainable from NASA, Washington

1. Heat Transfer, Aerodynamic (1.1.4.2)
 2. Wings, Complete (1.2.2)
 3. Wings, Complete - Design Variables (1.2.2.2)
 4. Wings, Complete - Sweep (1.2.2.2.3)
 5. Dihedral - Complete Wings (1.2.2.2.7)
- I. Stainback, P. Calvin
II. NASA TM X-247

NASA

NASA TM X-247

National Aeronautics and Space Administration.
PRELIMINARY HEAT-TRANSFER MEASUREMENTS
ON A HYPERSONIC GLIDE CONFIGURATION HAVING
79.5° SWEEPBACK AND 45° DIHEDRAL AT A MACH
NUMBER OF 4.95. P. Calvin Stainback. February
1960. 28p. diags., photos., tab.
(NASA TECHNICAL MEMORANDUM X-247)

(Title, Unclassified)
An experimental investigation was conducted to evaluate the heat-transfer characteristics of the configuration. The tests were conducted at a nominal Mach number of 4.95 and a stagnation temperature of 400° F. The test-section unit Reynolds number was varied from 1.95×10^6 to 12.24×10^6 per foot. The heat-transfer distribution (local heating rate relative to the ridge-line heating rate) and the ridge-line heat-transfer level could be predicted by two-dimensional blunt-body theory for angles of attack greater than 0° provided it was assumed that the stagnation line was located on the ridge line.
Copies obtainable from NASA, Washington

1. Heat Transfer, Aerodynamic (1.1.4.2)
 2. Wings, Complete (1.2.2)
 3. Wings, Complete - Design Variables (1.2.2.2)
 4. Wings, Complete - Sweep (1.2.2.2.3)
 5. Dihedral - Complete Wings (1.2.2.2.7)
- I. Stainback, P. Calvin
II. NASA TM X-247

NASA

031712001030

ERRATA

NASA Technical Memorandum X-247

By P. Calvin Stainback
February 1960

An error in calculating the theoretical stagnation-line heat-transfer rates given in table I invalidates the results presented in figure 3 and the discussion related thereto. The corrections are simplified somewhat when these results are presented in terms of the heat-transfer coefficients instead of the heating rates. Such a correction has been made, and the necessary changes are listed in the errata which follow:

Page 1: Replace last sentence of paragraph 2 (lines 9 to 14) with the following sentence:

Except in the vicinity of the apex, the ridge-line heat-transfer level could also be predicted from two-dimensional blunt-body heat-transfer theory provided it was assumed that the stagnation-line heat-transfer coefficient varied as the cosine of the effective sweep (sine of the angle of attack of the ridge line).

Page 2: Add to definition for h the following:

h model height (inches) in section on model description; elsewhere, aerodynamic heat-transfer coefficient, $\text{Btu}/\text{sec}\text{-ft}^2\text{-}^\circ\text{F}$

Page 4: Add following symbol to list of subscripts:

w value at wall

Page 6:

In line 24, change "heating rate" to "heat-transfer coefficient."

In line 26, change "heat-transfer rate" to "heat-transfer coefficient."

In line 27, change "heat-transfer rate" to "heat-transfer coefficient."

In line 31, change "The data were reduced . . ." to "The heat-transfer-distribution data were reduced . . ."

THIS PAGE IS UNCLASSIFIED

Issued August 4, 1960, Page 1 of 8

REF ID: A66571

THIS PAGE IS UNCLASSIFIED

- 2 -

Page 9, lines 22 to 38: Replace paragraphs 4 and 5 with the following:

Figure 3 presents the ratio of the measured stagnation-line heat-transfer coefficient to the theoretical value, $h/h_{sl,th}$, where $h_{sl,th}$ was calculated from the results of reference 5 and the cosine relationship of reference 6. The theoretical stagnation-line heat-transfer coefficients are tabulated in table I for reference. For most conditions investigated, the theoretical heat-transfer coefficient overestimated the heat-transfer coefficient for the ridge line except in the vicinity of the apex. This overestimation was as much as 35 percent, but the average was of the order of 15 percent. The high heating rate in the vicinity of the apex agrees with the trend which could be predicted from the measured pressure data of reference 8.

Figure 3 also presents the ratio of the heat-transfer coefficient for the center line of the upper surface of the model to the theoretical ridge-line (stagnation-line) heat-transfer coefficient. The laminar-flow heat-transfer coefficient for the upper-surface center line was about 20 percent of the theoretical ridge-line heat-transfer coefficient except for an angle of attack $\alpha' = 0^\circ$.

Page 11, lines 13 to 18: Replace last sentence with following:

Except in the vicinity of the apex, the ridge-line heat-transfer level could also be predicted from two-dimensional blunt-body heat-transfer theory provided it was assumed that the stagnation-line heat-transfer coefficient varied as the cosine of the effective sweep (sine of the angle of attack of the ridge line).

Page 13: Replace table I with revised table I attached.

Pages 20-24: Replace figures 3(a) to 3(e) with revised figures 3(a) to 3(e) attached.

THIS PAGE IS UNCLASSIFIED

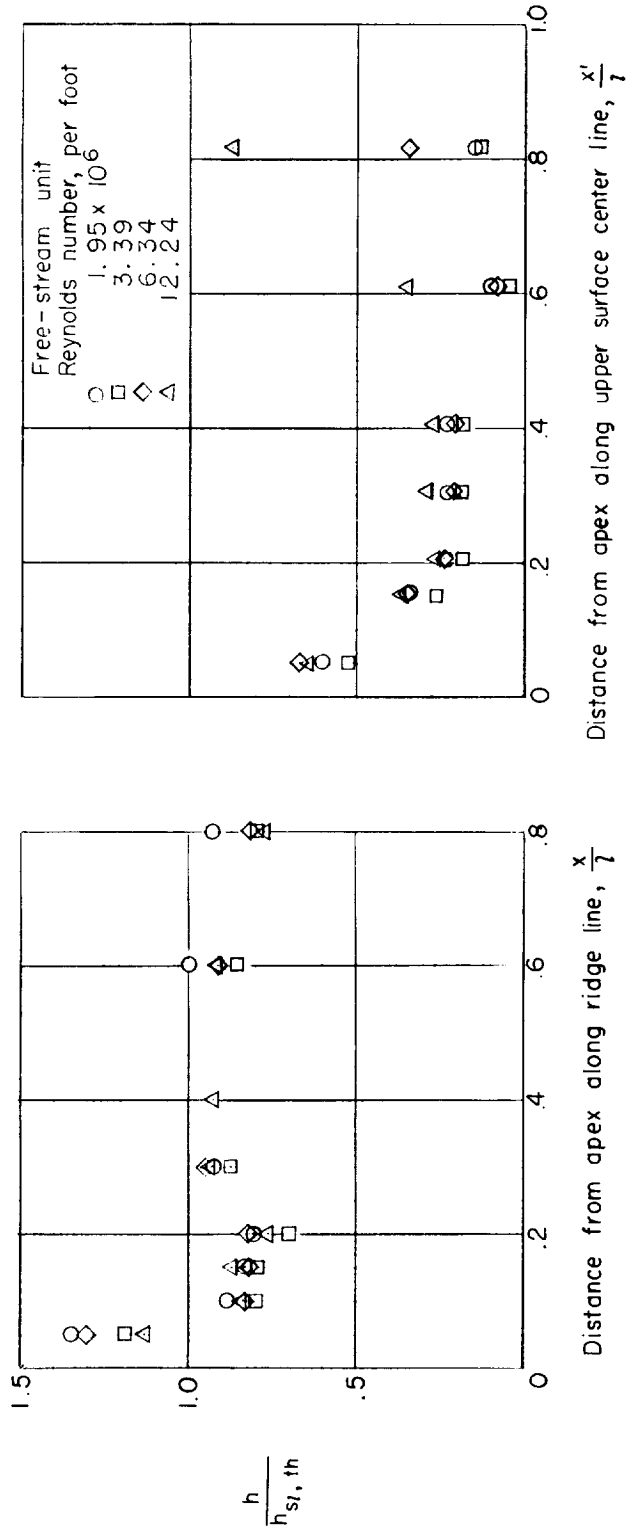
Issued August 4, 1960, Page 2 of 8

TABLE I
 THEORETICAL STAGNATION-LINE (RIDGE-LINE) HEAT-TRANSFER COEFFICIENTS

[M = 4.95; T_t = 400° F; r = 0.50 in.; T_w = 75° F]

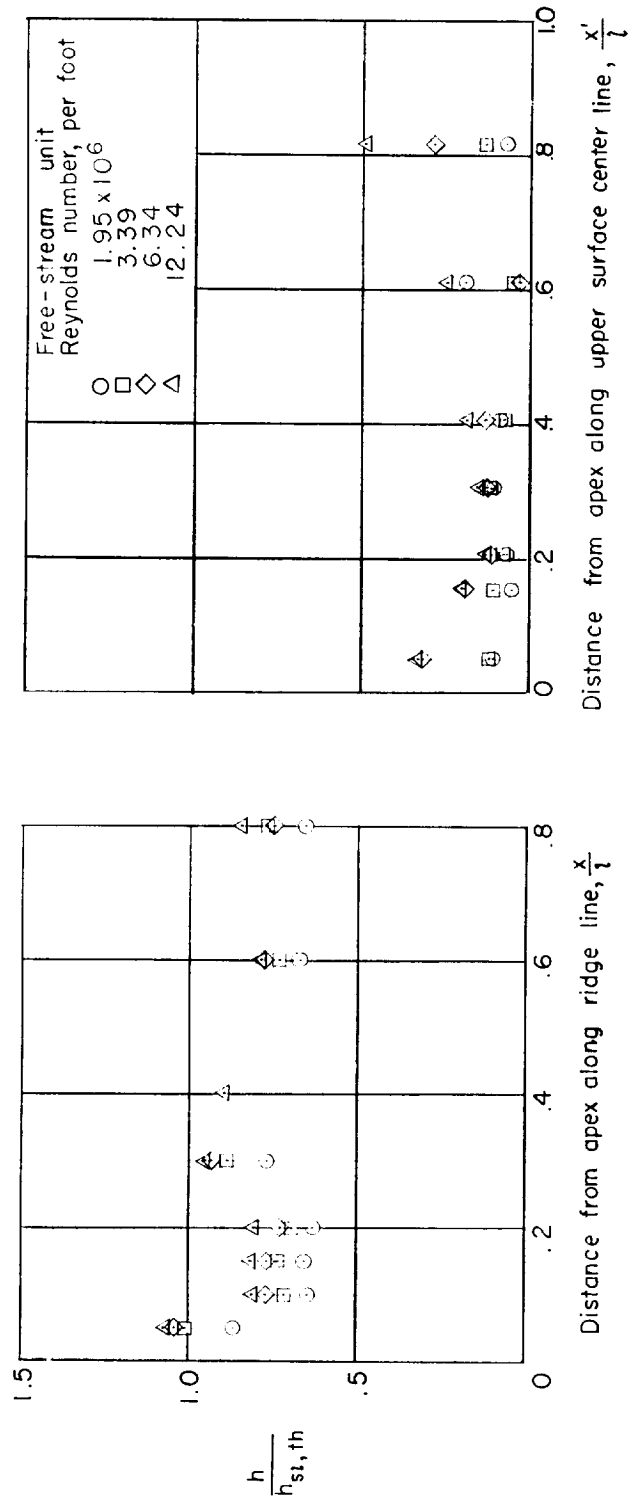
N _{Re} per foot	h _{sl,th} , Btu/sec-ft ² -°F, at -				
	α' = 0°	α' = 5°	α' = 10°	α' = 15°	α' = 20°
1.95 × 10 ⁶	0.00307	0.00448	0.00585	0.00717	0.00844
3.39	.00409	.00596	.00778	.00954	.01124
6.34	.00559	.00814	.01064	.01305	.01536
12.24	.00776	.01131	.01478	.01813	.02135

REF ID: A60000



(a) $\alpha' = 0^\circ$.

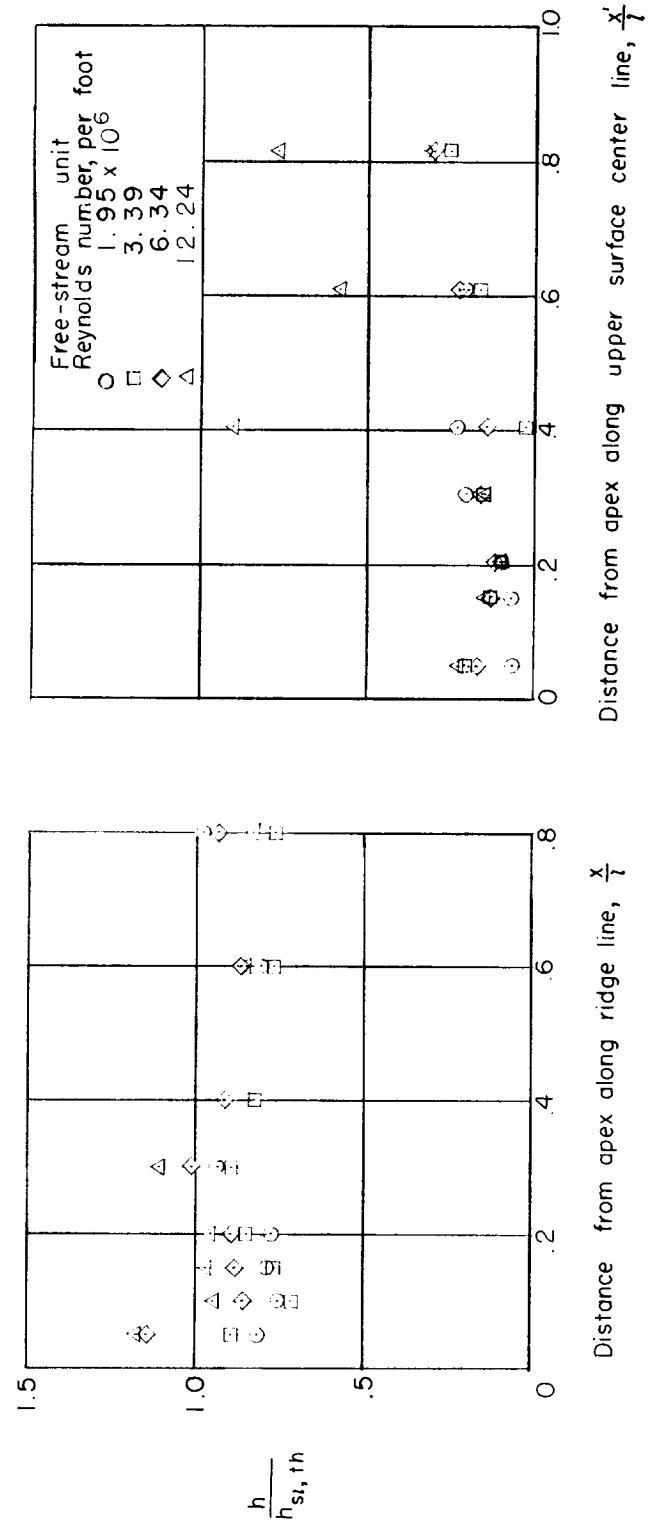
Figure 3.- Heat transfer to model along ridge line and upper-surface center line.



(b) $\alpha' = 5^\circ$.

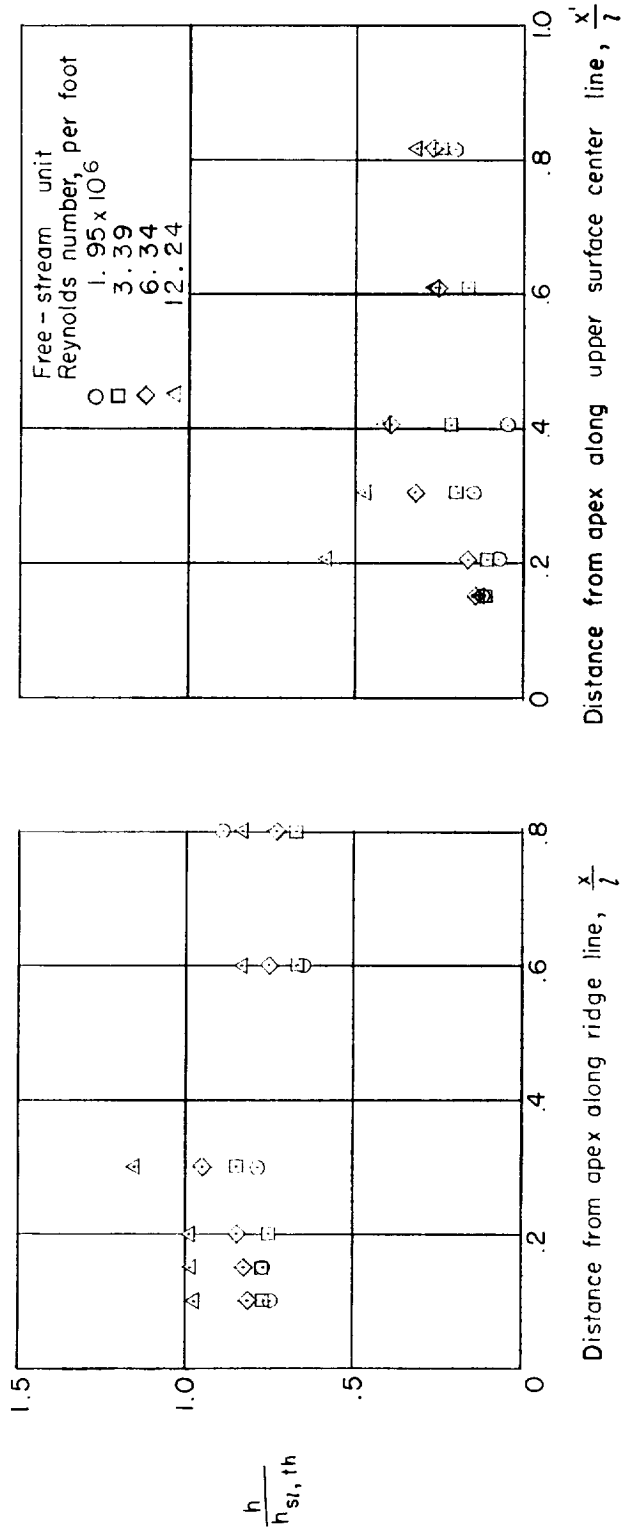
Figure 3.- Continued.

RESEARCH



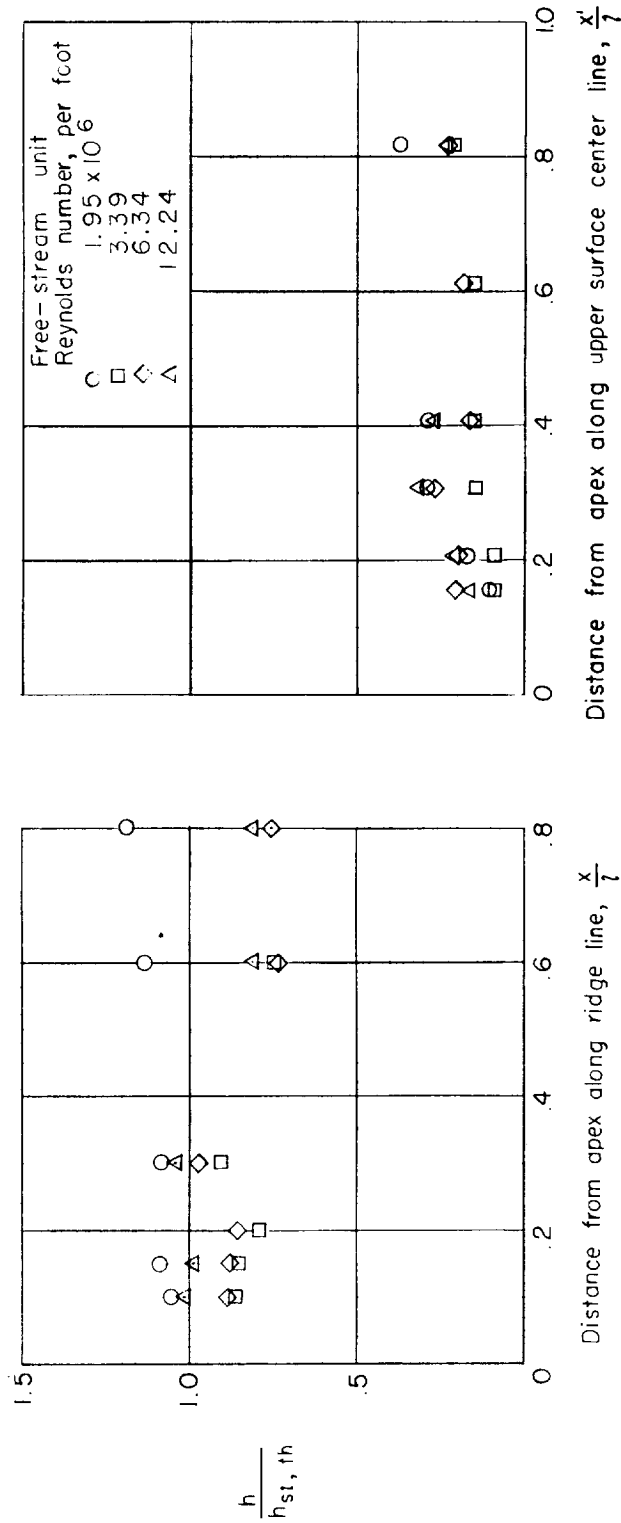
(c) $\alpha' = 10^\circ$.

Figure 3.- Continued.



(a) $\alpha' = 15^\circ$.

Figure 3.- Continued.



(e) $\alpha' = 20^\circ$.

Figure 3.- Concluded.

